JACS
JOURNAL OF THE AMERICAN CHEMICAL SOCIETY
pubs.acs.org/JACS
Communication

Expanding Reaction Profile of Allyl Carboxylates via 1,2-Radical Migration (RaM): Visible-Light-Induced Phosphine-Catalyzed 1,3-Carbobromination of Allyl Carboxylates

Gaoyuan Zhao, Sanghyun Lim, Djamaladdin G. Musaev,* and Ming-Yu Ngai*

Cite This: https://doi.org/10.1021/jacs.2c11867
Read Online
ACCESS | Metrics & More | Article Recommendations | Supporting Information

ABSTRACT: Allyl carboxylates are useful synthetic intermediates in a variety of organic transformations, including catalytic nucleophilic/electrophilic allylic substitution reactions and 1,2-difunctionalization reactions. However, the catalytic 1,3-difunctionalization of allyl carboxylates remains elusive. Herein, we report the first photoinduced, phosphine-catalyzed 1,3-carbobromination of allyl carboxylates, affording a range of valuable substituted isopropyl carboxylates (sIPC). The transformation has broad functional group tolerance, is amenable to the late-stage modification of complex molecules and gram-scale synthesis, and expands the reaction profiles of allyl carboxylates and phosphine catalysis. Preliminary experimental and computational studies suggest a non-chain-radical mechanism involving the formation of an electron donor–acceptor complex, 1,2-radical migration (RaM), and Br-atom transfer processes. We anticipate that the 1,2-RaM reactivity of allyl carboxylates and the phosphine-catalyzed radical reaction will both serve as a platform for future new transformations in organic synthesis.

Allyl carboxylates are versatile synthetic intermediates that can be applied to a wide spectrum of reliable derivatizations. For example, they can participate in transition-metal (TM)-catalyzed two-electron redox reactions (Figure 1A), which often proceed through TM-π-allyl intermediates that react with nucleophiles[1] or electrophiles,[2] generating a wide array of allylated organic compounds. The olefin moiety of allyl carboxylates can also engage in one-electron redox reactions with radical species to form alkyl radical intermediates that partake in cross-coupling reactions, furnishing valuable 1,2-difunctionalized products.[3] Despite these advances, catalytic radical 1,3-difunctionalization of allyl carboxylates involving 1,2-radical migration (RaM) remains elusive.[4] Inspired by the Surzur–Tanner rearrangement, in which a β-(acyloxy)alkyl radical undergoes 1,2-RaM via an acyloxy shift to form a more stable radical intermediate,[5] we questioned whether we could achieve the catalytic radical 1,3-difunctionalization of allyl carboxylates via a 1,2-RaM mechanism. If successful, this new reaction manifold could serve as the basis for a broadly useful set of allyl carboxylate derivatization protocols that support the preparation of a wide variety of versatile building blocks for synthesis, medicinal, and material chemistry.

Phosphorus-based catalysis has emerged as a promising strategy in organic synthesis for the formation of carbon–carbon and carbon–heteroatom bonds.[6] In this area, the vast majority of the reactions, such as nucleophilic phosphine catalysis and phosphine oxide catalysis, take advantage of the two-electron redox reactivity of phosphorus compounds to generate ionic intermediates.[7] In contrast, phosphine-catalyzed one-electron pathways that generate radical species are underdeveloped.[6b,e,8] One approach to such reactions involves halogen-atom transfer (XAT) reactions[9] in which the highest occupied molecular orbital (HOMO) of phosphine (i.e., the lone pair electrons) interacts with the lowest unoccupied molecular orbital (LUMO) of the C–X bond (i.e., the antibonding orbital of the C–X bond), forming an electron donor–acceptor (EDA) complex.[10] Photoexcitation of these EDA complexes furnishes alkyl radicals and phosphine halide radicals. The pioneering work in this area was reported in 2019 by Czekelius, who developed visible-light-induced phosphine-catalyzed 1,2-difunctionalization of alkenes through XAT of iododifluoroacetates.[8e,11] In spite of these elegant works, activation of the corresponding bromodifluoroacetate derivatives through the same activation mode remains elusive. Presumably, this is due to the higher LUMO energy level of bromodifluoroacetates,[12] weakening the HOMO–LUMO interaction (Table S1). DFT calculations show that ΔH of the $Me_3P\cdots Br$ EDA complex is −3.0 kcal/mol, which is higher than that of the $Me_3P\cdots I$ EDA complex (−6.7 kcal/mol, Figure 1B), but the negative enthalpic energy suggests that formation of the P···Br EDA complex may still be feasible. Accordingly, we hypothesized that merging phosphine-catalyzed XAT of polyfluoroalkyl bromides with a 1,2-RaM process would (i) enable the previously elusive 1,3-carbobromination of allyl carboxylates; (ii) expand the reaction profiles of allyl carboxylates and phosphine catalysis; (iii) produce organic compounds bearing the valuable gem-difluoromethylene pharmacophore;[13] and (iv) establish a new reaction platform

Received: November 7, 2022

https://doi.org/10.1021/jacs.2c11867
J. Am. Chem. Soc. XXXX, XXX, XXX−XXX

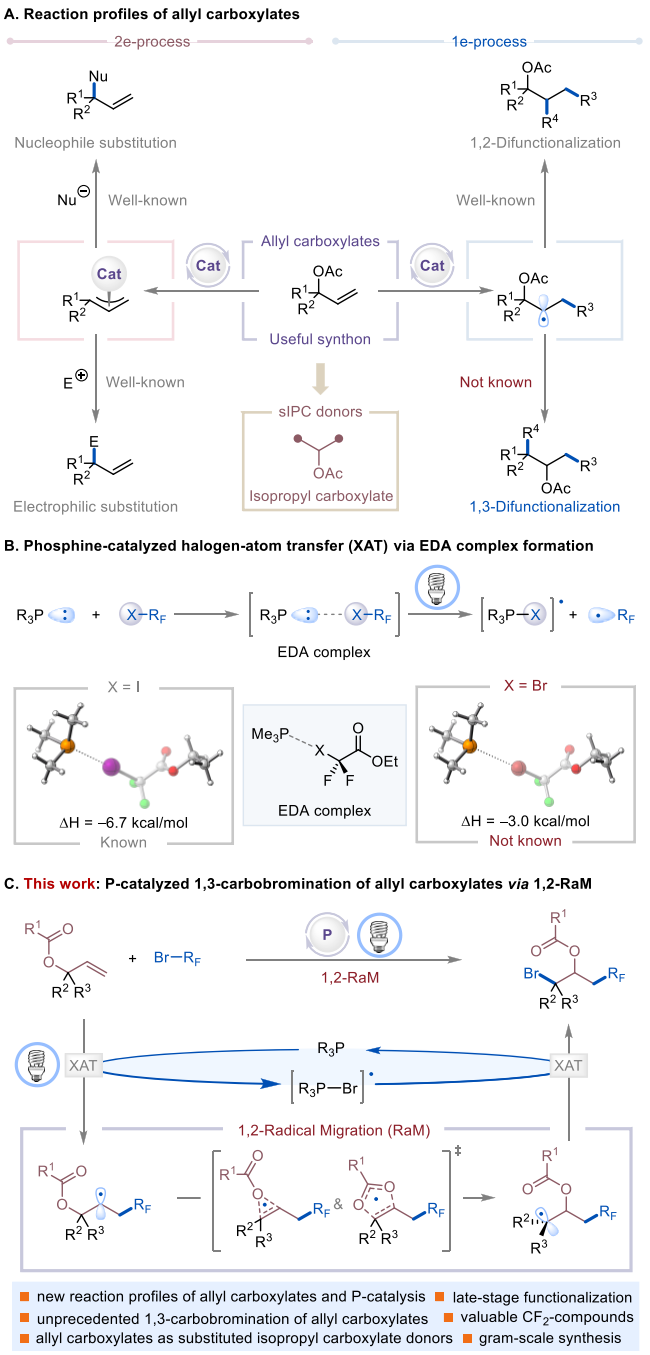

Figure 1. Reactions of allyl carboxylates and visible-light-induced phosphine-catalyzed 1,3-bromodifluoroalkylation of allyl carboxylates.

using allyl carboxylates as a substituted isopropyl carboxylate donor in organic synthesis (Figure 1C).

To test our hypothesis, we examined the reaction between allyl benzoate (**1a**) and ethyl bromodifluoroacetate (**2a**, Table 1). After some initial experimentation, we found that, upon exposing **1a** (1.00 equiv) and **2a** (3.00 equiv) to 100 W blue light-emitting diodes (LED) in the presence of 1,1-bis-(diphenylphosphino)methane (dppm, 10.0 mol %) and Na_2CO_3 (2.50 equiv) in 1,2-dichloroethane (DCE, 0.04 M) at 90 °C for 24 h, we obtained the desired 1,3-bromodifluoroalkylated product **3a** in 86% yield (entry 1). The dppm catalyst is essential for this reaction, since there was no reaction in its absence (entry 2). Other phosphine catalysts

Table 1. Selected Optimization Experiments[a,b]

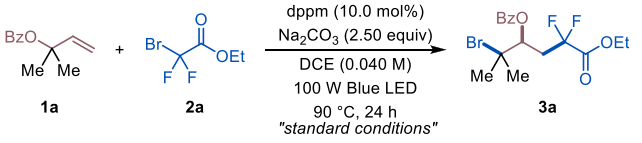

1a **2a** **3a**

entry	deviation from the standard conditions	yield (%)
1	none	86
2	no dppm	N.R.
3	Ph_3P instead of dppm	51
4	n-Bu_3P instead of dppm	60
5	BINAP instead of dppm	71
6	Eosin Y	10
7	$Ru(bpy)_3(PF_6)_2$	16
8	$Ir(ppy)_3$	72
9	no base	0
10	K_2CO_3 instead of Na_2CO_3	67
11	KOAc instead of Na_2CO_3	70
12	2,6-lutidine instead of Na_2CO_3	50
13	MeCN as solvent	68
14	room temperature	N.R.
15	no light	N.R.
16	with air	N.R.

[a]

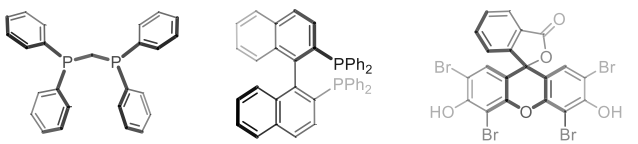

dppm BINAP Eosin Y

[b]See the Supporting Information for experimental details. Reaction yields were determined by ^1H NMR using CH_2Br_2 as an internal standard. Bz, benzoyl; BINAP, 2,2′-bis(diphenylphosphino)-1,1′-binaphthyl; LED, light-emitting diode; N.R., no reaction.

such as Ph_3P, *n*-Bu_3P, and 2,2′-bis(diphenylphosphino)-1,1′-binaphthyl (BINAP) gave lower yields (entries 3–5). While organic photocatalysts such as Eosin Y and a Ru-based photocatalyst were inefficient, the $Ir(ppy)_3$ photocatalyst afforded the desired product in 72% yield (entries 6–8). We proceeded with the dppm catalyst ($1.375/mmol) because it is more than 1000 times cheaper than $Ir(ppy)_3$ ($1,784/mmol).[14] Na_2CO_3 is critical for the reaction efficiency because no desired product was obtained in its absence (entry 9). Other inorganic and organic bases such as K_2CO_3, KOAc, and 2,6-lutidine could be used, but they afforded lower yields (entries 10–12).[15] Use of acetonitrile as the solvent also diminished the reaction yield (entry 13). Finally, control experiments showed that a temperature of 90 °C, light, and an oxygen-free environment were all essential to the success of the reaction (entries 14–16).

With the optimized conditions in hand, we investigated the scope of allyl carboxylates (Table 2). A series of substituted allyl carboxylates, including linear and cyclic frameworks, were well tolerated, affording the corresponding products **3a**–**3h** in 53–88% yield. Substrates containing cyclic ether, thioether (**3i** and **3j**), or the ethylene ketal group (**3k**) were also compatible. However, allyl carboxylates with a secondary alkyl substituent or internal alkene failed under standard reaction conditions. Next, we examined a wide range of migrating groups with different electron-donating and electron-withdrawing substituents at various positions of the aromatic ring, all of which

https://doi.org/10.1021/jacs.2c11867
J. Am. Chem. Soc. XXXX, XXX, XXX–XXX

Table 2. Visible-Light-Induced Phosphine-Catalyzed 1,3-Bromodifluoroalkylation of Allyl Carboxylates[a]

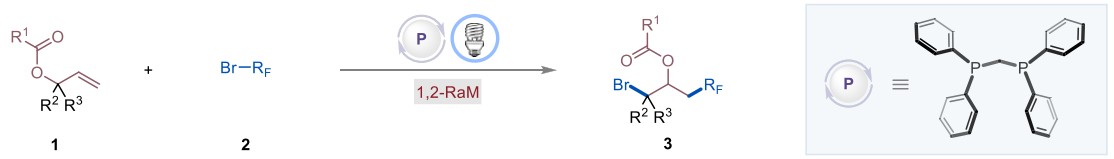

A. Allyl Carboxylates

3a, 80%

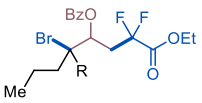

3b,R = *n*-Pr, 78%
3c,R = Me, 75%, dr 1:1

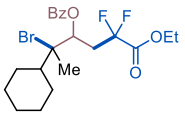

3d, 55%, dr 1:1

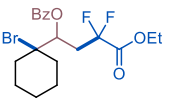

3e, 88%

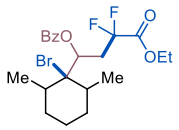

3f, 65%

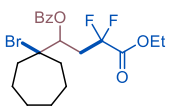

3g, 60%

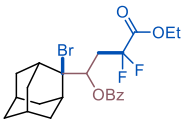

3h, 53%

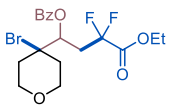

3i, 77%

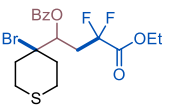

3j, 73%

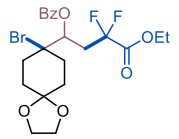

3k, 86%

B. Migrating Groups

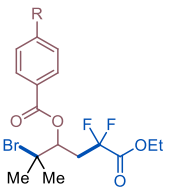

3l, R = *t*-Bu, 63%
3m, R = OMe, 63%

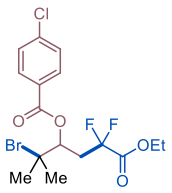

3n, 81%

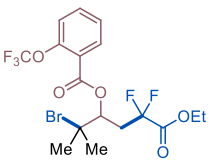

3o, 63%

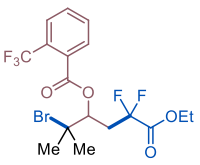

3p, 51%

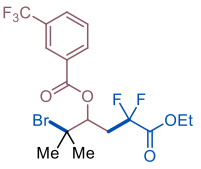

3q, 65%

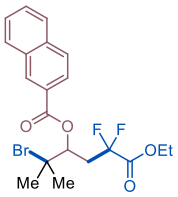

3r, 42%

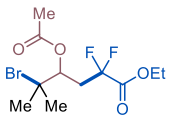

3s, 63%

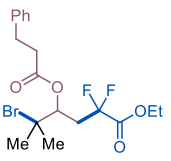

3t, 60%

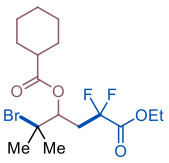

3u, 54%

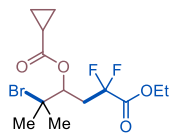

3v, 70%

C. Bromodifluoroalkyl Derivatives

3w, 65%

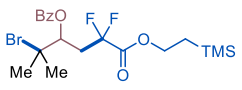

3x, 63%

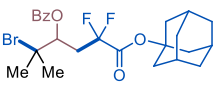

3y, 69%

3z, 54%

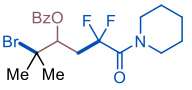

3aa, 71%

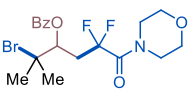

3ab, 79%

3ac, 61%

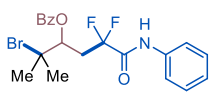

3ad, 73%

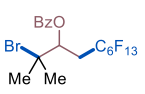

3ae, 67%[b]

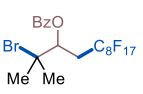

3af, 68%[b]

[a]See the Supporting Information for experimental details; **1** (1.00 equiv), **2** (3.00 equiv), dppm (10.0 mol %), Na_2CO_3 (2.50 equiv), DCE (0.040 M), 100 W blue LED, 90 °C, 24 h. [b]5.00 equiv of BrC_6F_{13} or BrC_8F_{17} was used and reacted for 48 h.

underwent 1,3-bromodifluoroalkylation in 51−81% yield (**3l**−**3q**). Allyl carboxylates with *ortho*-, *meta*-, and *para*-substituted benzoate substituent migrating groups reacted with similar efficiency. 2-Naphthoates and aliphatic esters also migrated successfully, affording the desired products **3r**−**3v** in moderate to good yields. Furthermore, we demonstrated that alternative primary, secondary, and tertiary ester substituents on the bromodifluoroacetates worked well and delivered **3w**−**3y** in 63−69% yield. An array of bromodifluoroacetamides such as *N*-diethyl, piperidinyl, morpholinyl, *N*-adamantyl, and *N*-

https://doi.org/10.1021/jacs.2c11867
J. Am. Chem. Soc. XXXX, XXX, XXX−XXX

phenyl bromodifluoroacetamides were viable substrates, producing the corresponding products **3z**–**3ad** in 54–79% yield. Finally, bromoperfluoroalkanes were also competent under this protocol (**3ae** and **3af**).

Late-stage modification of bioactive complex molecules is a pragmatic means to discover new medicinal agents.[16] To demonstrate the applicability of the visible-light-induced phosphine-catalyzed 1,3-bromodifluoroalkylation to late-stage diversifications, natural-product- and drug-conjugated substrates were subjected to the standard reaction conditions (Table 3). For example, probenecid (a drug that prevents gout) and cholic acid-derived allyl carboxylates reacted under standard conditions, affording the desired products **3ag** and **3ah** in 79% and 53% yield, respectively. Riluzole (an amyotrophic lateral sclerosis drug)-derived bromodifluoroacetamide also participates in this transformation (**3ai**). Bromodifluoroacetate derivatives of vitamin E, L-menthol (a decongestant and analgesic), diactonefructose, diacetone-D-glucose, and diosgenin worked well under the standard conditions, forming the desired products **3aj**–**3an** in 48–84% yield.

To showcase the scalability of this process, a gram-scale reaction was performed by using substrates **1a** and **2a** (Scheme 1A). A satisfactory 82% isolated yield of **3a** was obtained under the irradiation of two 100 W blue LEDs for 72 h. We also performed a series of transformations to demonstrate the synthetic utility of the 1,3-bromodifluoroalkylated products in forming useful molecular scaffolds (Scheme 1B). The bromine and ester functionality in the product could be used for subsequent synthetic manipulations. For example, selective HBr elimination was achieved in the presence of the benzoate leaving group, generating the useful terminal alkene **4**. The synthetic utility of the ester was exemplified by selective reduction, hydrolysis, and amidation of the ethyl ester without affecting the alkyl benzoate, furnishing the corresponding alcohol **5**, acid **6**, and amide **7** in 76%, 62%, and 94% yields, respectively.

To gain a better understanding of the reaction mechanism, we carried out a series of experimental and computational studies (Figure 2). The addition of 2,2,6,6-tetramethylpiperidine 1-oxyl (TEMPO) as a radical scavenger significantly inhibited the reaction (Figure 2A). The TEMPO-trapped difluoroacetate adduct (**8**) was isolated and characterized by NMR and HRMS spectrometry. A radical clock experiment using substrate **1ao** formed the ring-opening product **3ao** in 42% yield. These experiments suggest a radical mechanism. We then subjected 1,2-bromodifluoroalkylated compound **9** to the standard conditions (Figure 2B). We did not obtain the desired 1,3-product, indicating that the reaction does not proceed through 1,2-bromodifluoroalkylation followed by ionic translocation of the benzoate and bromide groups. Crossover experiments using substrates **1s** and **1e** furnished only the non-crossover products **3s** and **3e**, respectively, implying that the acyloxy shift probably proceeds through concerted mechanisms (Figure 2C).[18] The O^{18}-labeling experiment using **1-O^{18}**

Table 3. Late-Stage Modification of Complex Molecules[a]

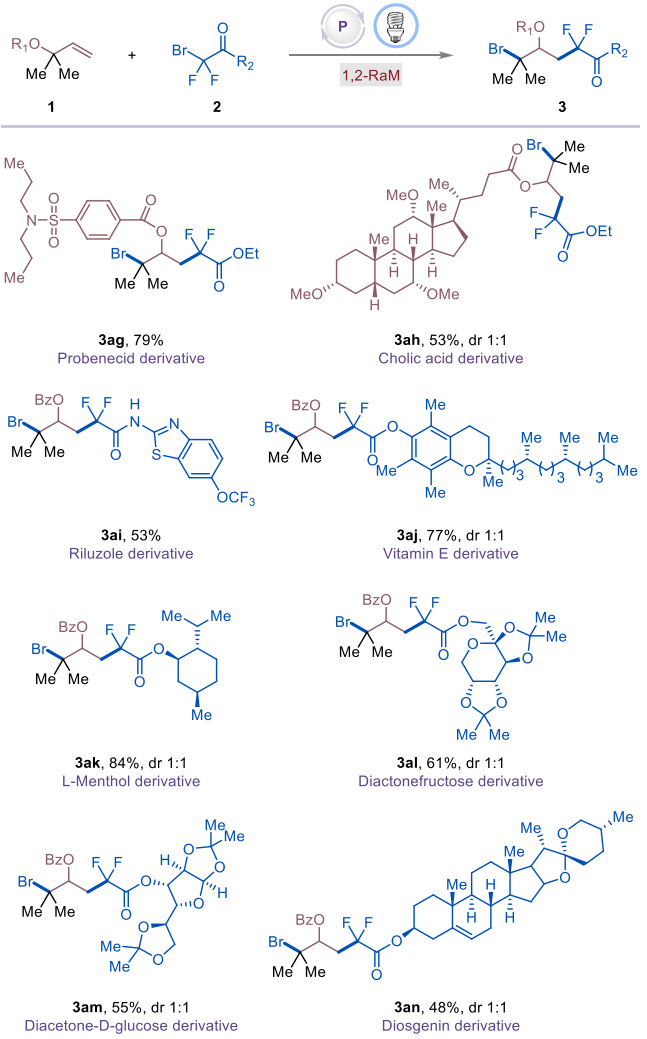

[a]See the Supporting Information for experimental details; **1** (1.00 equiv), **2** (3.00 equiv), dppm (10.0 mol %), Na_2CO_3 (2.50 equiv), DCE (0.040 M), 100 W blue LED, 90 °C, 24 h.

Scheme 1. Large-Scale Reaction and Post-Functionalization[a]

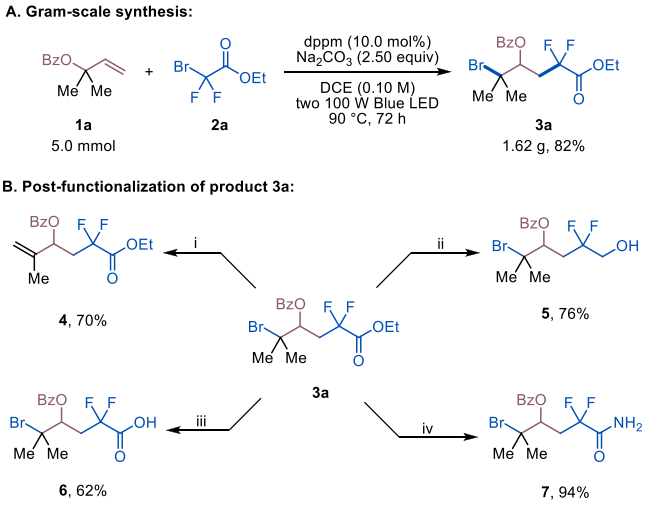

[a]See the Supporting Information for experimental details. (i) DBU (1.50 equiv), DMSO (0.200 M), 60 °C, 6 h; (ii) $NaBH_4$ (2.00 equiv), MeOH (0.200 M), 0 °C to rt, 3 h; (iii) K_2CO_3 (5.00 equiv), MeOH/H_2O (1:1, 0.100 M), rt, 12 h; (iv) NH_3 (10.0 equiv), MeOH (0.100 M), rt, 16 h.

https://doi.org/10.1021/jacs.2c11867
J. Am. Chem. Soc. XXXX, XXX, XXX–XXX

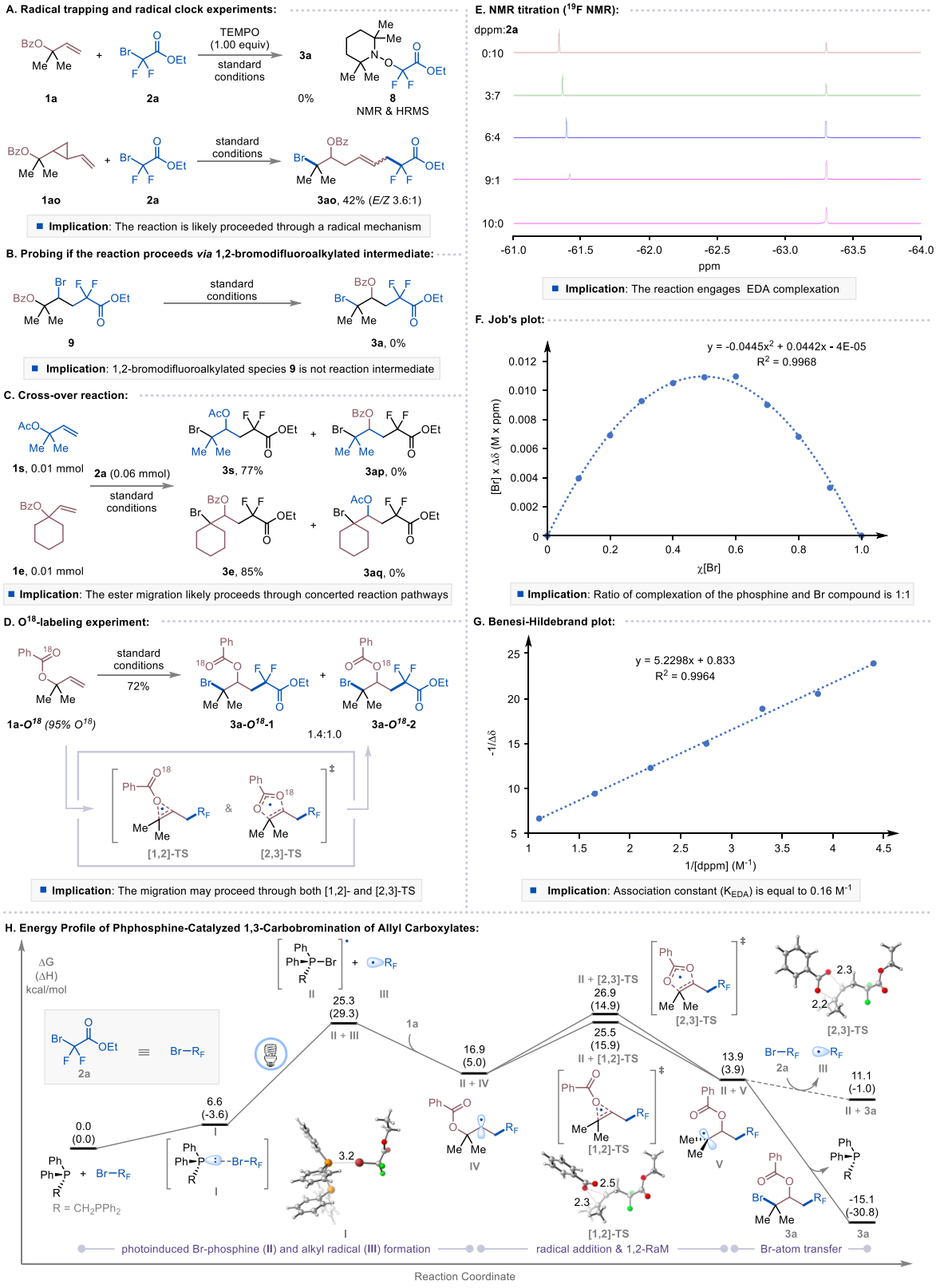

Figure 2. Mechanistic studies. All energies are in kcal/mol and are relative to dppm and **2a**. Distances between the critical atoms are given in Å (see the Supporting Information for details). The 3D representation was prepared by using CYLview.[17]

with 95% O^{18} incorporation afforded the products **3a-O^{18}-1** and **3a-O^{18}-2** in a 1.4:1 ratio, indicating that both [1,2]- and [2,3]-acyloxy group shift pathways may operate simultaneously (Figure 2D).[19] Light on/off experiments and quantum yield measurement (ϕ = 0.0029) suggested that an extended radical chain mechanism is unlikely (Figures S4 and S7).

To elucidate the role of dppm in this reaction, we performed ^{19}F NMR titration experiments, which showed an upfield shift

https://doi.org/10.1021/jacs.2c11867
J. Am. Chem. Soc. XXXX, XXX, XXX−XXX

as the concentration of dppm increased (Figure 2E). This observation suggests the donation of phosphine lone-pair electrons into the anti-bonding orbital of the C−Br bond of **2a**, which increases the electron density at the α-carbon and shields the fluorine atoms. The Job's plot[20] and Benesi−Hildebrand plot[21] revealed the formation of a 1:1 dppm−**2a** complex with an association constant (K_{EDA}) of 0.16 M^{-1} (Figure 2F and G).

The precise photoexcitation mechanism remains elusive because the UV−vis measurements of a mixture of dppm and **2a** in DCE showed no visible changes in the absorption compared to individual components (Figure S17). Nevertheless, DFT and TD-DFT calculations revealed that (i) the formation of the dppm−**2a** complex (**I**) is enthalpically favored by −3.6 kcal/mol and is endergonic by only 6.6 kcal/mol (Figure 2H) and (ii) different conformers of complex **I** and their Na_2CO_3 adducts have absorptions extending into the visible light region (Figures S14−S16).[22,23] These conformers and adducts are higher in energy and may exist at concentrations outside the detection limit of the UV−vis spectrometer.

DFT calculations showed that [**1,2**]-**TS** is 1.4 kcal/mol lower than [**2,3**]-**TS** in terms of Gibbs free energy but 1.0 kcal/mol higher in terms of enthalpy. Thus, the preference of one over another is the subject of entropy corrections and, consequently, experimental conditions (Figure 2H). The Br-atom transfer from bromophosphine radical intermediate **II** to **V** is highly exergonic (−29.0 kcal/mol) with ∼4.4 kcal/mol energy barrier at the minimum on the triplet and singlet state (i.e., T/S) seam of crossing (MSX), liberating the phosphine catalyst and product **3a** (Figure S19). Thus, this process is more favorable than the alternative radical chain reaction, which is exergonic only by 2.8 kcal/mol but has an energy barrier of 17.7 kcal/mol (Figure S20). Nevertheless, we cannot completely rule out the radical chain mechanism in this stage.

Although we do not have a complete mechanistic understanding of the photoexcitation process, a plausible catalytic cycle is outlined in Figure 3. Photoexcitation of complex **I** or its Na_2CO_3 adducts generates bromophosphine radical species **II** and difluoroalkyl radical **III**.[8e,11] Subsequent radical addition of **III** to allyl benzoate **1a** affords the secondary alkyl radical **IV**. Intermediate **IV** undergoes concerted [1,2]- and [2,3]-benzoyloxy shifts ([**1,2**]-**TS** and [**2,3**]-**TS**),[5] forming the more stable tertiary radical intermediate **V**. Finally, Br-atom transfer from bromophosphine species **II** (or **2**) to radical intermediate **V** delivers the desired product **3** and regenerates dppm, closing the catalytic cycle.[24]

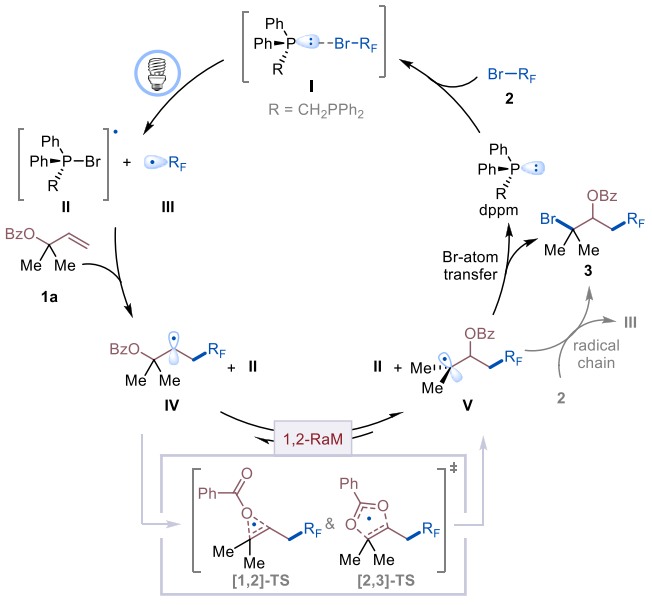

Figure 3. Proposed reaction mechanism.

In summary, we have developed the first visible-light-induced phosphine-catalyzed 1,3-carbobromination of allyl carboxylates, expanding the reaction profiles of allyl carboxylates and phosphine catalysis. The reaction forms a series of valuable 1,3-bromodifluoroalkylated products, tolerates a wide array of functional groups, and is amenable to late-stage modification of complex molecules and gram-scale synthesis. Preliminary mechanistic studies suggest a non-chain-radical mechanism involving the formation of dppm−**2a** complexes, 1,2-RaM, and Br-atom transfer processes. We anticipate that the 1,2-RaM reactivity of allyl carboxylates and phosphine-catalyzed radical reaction will provide a pathway for the development of new chemical transformations in organic synthesis.

■ ASSOCIATED CONTENT

Supporting Information

The Supporting Information is available free of charge at https://pubs.acs.org/doi/10.1021/jacs.2c11867.

Experimental details and characterization data for all new compounds (PDF)

■ AUTHOR INFORMATION

Corresponding Authors

Djamaladdin G. Musaev − *Cherry L. Emerson Center for Scientific Computation, and Department of Chemistry, Emory University, Atlanta, Georgia 30322, United States;* orcid.org/0000-0003-1160-6131; Email: dmusaev@emory.edu

Ming-Yu Ngai − *Department of Chemistry and Institute of Chemical Biology and Drug Discovery, State University of New York, Stony Brook, New York 11794, United States;* orcid.org/0000-0002-3055-6662; Email: ming-yu.ngai@stonybrook.edu

Authors

Gaoyuan Zhao − *Department of Chemistry, State University of New York, Stony Brook, New York 11794, United States;* orcid.org/0000-0003-4838-865X

Sanghyun Lim − *Department of Chemistry, State University of New York, Stony Brook, New York 11794, United States*

Complete contact information is available at: https://pubs.acs.org/10.1021/jacs.2c11867

Notes

The authors declare no competing financial interest.

■ ACKNOWLEDGMENTS

This paper is dedicated to Professor Albert Padwa on the occasion of his 85th birthday. M.-Y.N. thanks the National Science Foundation (CHE1848463) for supporting this research. D.G.M. acknowledges the support of the National Science Foundation under the CCI Center for Selective C−H Functionalization (CHE-1700982) and the use of the

resources of the Cherry Emerson Center for Scientific Computation at Emory University. The Shimadzu UPLC/MS used for portions of this work was purchased with funds from NIGMS equipment administrative supplement (R35-GM119652-04S1), Shimadzu Scientific Instruments grant, and Office of the Vice President for Research at Stony Brook University. We thank Professors Jayaraman Sivaguru and Rui Shang for the fruitful discussion on photoexcitation chemistry and the reviewers' insightful comments and suggestions.

■ REFERENCES

(1) For selected reviews and accounts, see: (a) Trost, B. M.; Van Vranken, D. L. Asymmetric Transition Metal-Catalyzed Allylic Alkylations. *Chem. Rev.* **1996**, *96*, 395−422. (b) Trost, B. M.; Crawley, M. L. Asymmetric Transition-Metal-Catalyzed Allylic Alkylations: Applications in Total Synthesis. *Chem. Rev.* **2003**, *103*, 2921−2944. (c) Mohr, J. T.; Stoltz, B. M. Enantioselective Tsuji Allylations. *Chem. Asian J.* **2007**, *2*, 1476−1491. (d) Hartwig, J. F.; Stanley, L. M. Mechanistically Driven Development of Iridium Catalysts for Asymmetric Allylic Substitution. *Acc. Chem. Res.* **2010**, *43*, 1461−1475. (e) Hartwig, J. F.; Pouy, M. J. Iridium-Catalyzed Allylic Substitution. *Iridium Catalysis* **2011**, *34*, 169−208. (f) Weaver, J. D.; Recio, A., III; Grenning, A. J.; Tunge, J. A. Transition Metal-Catalyzed Decarboxylative Allylation and Benzylation Reactions. *Chem. Rev.* **2011**, *111*, 1846−1913. (g) Qu, J.; Helmchen, G. n. Applications of Iridium-Catalyzed Asymmetric Allylic Substitution Reactions in Target-Oriented Synthesis. *Acc. Chem. Res.* **2017**, *50*, 2539−2555. (h) Cheng, Y.; Mueck-Lichtenfeld, C.; Studer, A. Transition Metal-Free 1,2-Carboboration of Unactivated Alkenes. *J. Am. Chem. Soc.* **2018**, *140*, 6221−6225. (i) Dutta, S.; Bhattacharya, T.; Werz, D. B.; Maiti, D. Transition-Metal-Catalyzed C−H Allylation Reactions. *Chem.* **2021**, *7*, 555−605. For selected examples, see: (j) Trost, B. M.; Strege, P. E. Asymmetric Induction in Catalytic Allylic Alkylation. *J. Am. Chem. Soc.* **1977**, *99*, 1649−1651. (k) Hethcox, J. C.; Shockley, S. E.; Stoltz, B. M. Iridium-Catalyzed Diastereo-, Enantio-, and Regioselective Allylic Alkylation with Prochiral Enolates. *ACS Catal.* **2016**, *6*, 6207−6213. (l) Zhang, H. H.; Zhao, J. J.; Yu, S. Enantioselective Allylic Alkylation with 4-Alkyl-1,4-Dihydro-Pyridines Enabled by Photoredox/Palladium Co catalysis. *J. Am. Chem. Soc.* **2018**, *140*, 16914−16919. (m) Fujita, T.; Yamamoto, T.; Morita, Y.; Chen, H.; Shimizu, Y.; Kanai, M. Chemo- and Enantioselective Pd/B Hybrid Catalysis for the Construction of Acyclic Quaternary Carbons: Migratory Allylation of O-Allyl Esters to A-C-Allyl Carboxylic Acids. *J. Am. Chem. Soc.* **2018**, *140*, 5899−5903. (n) Jiang, R.; Ding, L.; Zheng, C.; You, S.-L. Iridium-Catalyzed Z-Retentive Asymmetric Allylic Substitution Reactions. *Science* **2021**, *371*, 380−386.

(2) For selected reviews and accounts, see: (a) Yus, M.; Gonzalez-Gomez, J. C.; Foubelo, F. Catalytic Enantioselective Allylation of Carbonyl Compounds and Imines. *Chem. Rev.* **2011**, *111*, 7774−7854. (b) Hassan, A.; Krische, M. J. Unlocking Hydrogenation for C−C Bond Formation: A Brief Overview of Enantioselective Methods. *Org. Process Res. Dev.* **2011**, *15*, 1236−1242. (c) Kim, S. W.; Zhang, W.; Krische, M. J. Catalytic Enantioselective Carbonyl Allylation and Propargylation Via Alcohol-Mediated Hydrogen Transfer: Merging the Chemistry of Grignard and Sabatier. *Acc. Chem. Res.* **2017**, *50*, 2371−2380. For selected examples, see: (d) Vogt, M.; Ceylan, S.; Kirschning, A. Stereocontrolled Palladium-Catalysed Umpolung Allylation of Aldehydes with Allyl Acetates. *Tetrahedron* **2010**, *66*, 6450−6456. (e) Kim, I. S.; Ngai, M.-Y.; Krische, M. J. Enantioselective Iridium-Catalyzed Carbonyl Allylation from the Alcohol or Aldehyde Oxidation Level Using Allyl Acetate as an Allyl Metal Surrogate. *J. Am. Chem. Soc.* **2008**, *130*, 6340−6341. (f) Kim, I. S.; Ngai, M.-Y.; Krische, M. J. Enantioselective Iridium-Catalyzed Carbonyl Allylation from the Alcohol or Aldehyde Oxidation Level Via Transfer Hydrogenative Coupling of Allyl Acetate: Departure from Chirally Modified Allyl Metal Reagents in Carbonyl Addition. *J. Am. Chem. Soc.* **2008**, *130*, 14891−14899. (g) Kim, I. S.; Han, S. B.; Krische, M. J. Anti-Diastereo-and Enantioselective Carbonyl Crotylation from the Alcohol or Aldehyde Oxidation Level Employing a Cyclometallated Iridium Catalyst: A-Methyl Allyl Acetate as a Surrogate to Preformed Crotylmetal Reagents. *J. Am. Chem. Soc.* **2009**, *131*, 2514−2520. (h) Lu, Y.; Kim, I. S.; Hassan, A.; Del Valle, D. J.; Krische, M. J. 1,N-Glycols as Dialdehyde Equivalents in Iridium-Catalyzed Enantioselective Carbonyl Allylation and Iterative Two-Directional Assembly of 1,3-Polyols. *Angew. Chem., Int. Ed.* **2009**, *48*, 5018−5021. (i) Han, S. B.; Gao, X.; Krische, M. J. Iridium-Catalyzed Anti-Diastereo-and Enantioselective Carbonyl (Trimethylsilyl) Allylation from the Alcohol or Aldehyde Oxidation Level. *J. Am. Chem. Soc.* **2010**, *132*, 9153−9156. (j) Gao, X.; Zhang, Y. J.; Krische, M. J. Iridium-Catalyzed Anti-Diastereo- and Enantioselective Carbonyl (Alpha-Trifluoromethyl)Allylation from the Alcohol or Aldehyde Oxidation Level. *Angew. Chem., Int. Ed.* **2011**, *50*, 4173−4175. (k) Gao, X.; Han, H.; Krische, M. J. Direct Generation of Acyclic Polypropionate Stereopolyads Via Double Diastereo-and Enantioselective Iridium-Catalyzed Crotylation of 1, 3-Diols: Beyond Stepwise Carbonyl Addition in Polyketide Construction. *J. Am. Chem. Soc.* **2011**, *133*, 12795−12800. (l) Dechert-Schmitt, A. M. R.; Schmitt, D. C.; Krische, M. J. Protecting-Group-Free Diastereoselective C-C Coupling of 1, 3-Glycols and Allyl Acetate through Site-Selective Primary Alcohol Dehydrogenation. *Angew. Chem., Int. Ed.* **2013**, *52*, 3195−3198. (m) Moragas, T.; Cornella, J.; Martin, R. Ligand-Controlled Regiodivergent Ni-Catalyzed Reductive Carboxylation of Allyl Esters with Co2. *J. Am. Chem. Soc.* **2014**, *136*, 17702−17705.

(3) For selected reviews on radical alkyl difunctionalization, see: (a) Koike, T.; Akita, M. New Horizons of Photocatalytic Fluoromethylative Difunctionalization of Alkenes. *Chem.* **2018**, *4*, 409−437. (b) Jiang, H.; Studer, A. Intermolecular Radical Carboamination of Alkenes. *Chem. Soc. Rev.* **2020**, *49*, 1790−1811. (c) Engl, S.; Reiser, O. Copper-photocatalyzed ATRA reactions: concepts, applications, and opportunities. *Chem. Soc. Rev.* **2022**, *51*, 5287−5299. (d) Xi, J.-M.; Liao, W.-W. Radical Addition to C= C Bond Meets (1, n)-HAT: Recent Advances on Remote C (sp3)-H or C (sp2)-H Functionalization of Alkenes. *Org. Chem. Front.* **2022**, *9*, 4490−4506. (e) Liu, T.; Liu, J.; He, J.; Hong, Y.; Zhou, H.; Liu, Y.-L.; Tang, S. Recent Advances in Photoinduced Perfluoroalkylation Using Perfluoroalkyl Halides as the Radical Precursors. *Synthesis* **2022**, *54*, 1919−1938. (f) Cao, M.-Y.; Ren, X.; Lu, Z. Olefin Difunctionalizations Via Visible Light Photocatalysis. *Tetrahedron Lett.* **2015**, *56*, 3732−3742. (g) Courant, T.; Masson, G. Recent Progress in Visible-Light Photoredox-Catalyzed Intermolecular 1, 2-Difunctionalization of Double Bonds Via an Atra-Type Mechanism. *J. Org. Chem.* **2016**, *81*, 6945−6952. For selected examples, see: (h) He, J.; Chen, C.; Fu, G. C.; Peters, J. C. Visible-Light-Induced, Copper-Catalyzed Three-Component Coupling of Alkyl Halides, Olefins, and Trifluoromethylthiolate to Generate Trifluoromethyl Thioethers. *ACS Catal.* **2018**, *8*, 11741−11748. (i) Wallentin, C. J.; Nguyen, J. D.; Finkbeiner, P.; Stephenson, C. R. J. Visible Light-Mediated Atom Transfer Radical Addition Via Oxidative and Reductive Quenching of Photocatalysts. *J. Am. Chem. Soc.* **2012**, *134*, 8875−8884. (j) Wang, F.; Wang, D.; Mu, X.; Chen, P.; Liu, G. Copper-Catalyzed Intermolecular Trifluoromethylarylation of Alkenes: Mutual Activation of Arylboronic Acid and Cf3+ Reagent. *J. Am. Chem. Soc.* **2014**, *136*, 10202−10205. (k) Wu, Z.; Wang, D.; Liu, Y.; Huan, L.; Zhu, C. Chemo-and Regioselective Distal Heteroaryl Ipso-Migration: A General Protocol for Heteroarylation of Unactivated Alkenes. *J. Am. Chem. Soc.* **2017**, *139*, 1388−1391. (l) Yang, Y.; Song, R. J.; Ouyang, X. H.; Wang, C. Y.; Li, J. H.; Luo, S. Iron-Catalyzed Intermolecular 1,2-Difunctionalization of Styrenes and Conjugated Alkenes with Silanes and Nucleophiles. *Angew. Chem., Int. Ed.* **2017**, *56*, 7916−7919. (m) Ye, K.-Y.; Pombar, G.; Fu, N.; Sauer, G. S.; Keresztes, I.; Lin, S. Anodically Coupled Electrolysis for the Heterodifunctionalization of Alkenes. *J. Am. Chem. Soc.* **2018**, *140*, 2438−2441. (n) Tang, X.; Studer, A. Alkene 1,2-Difunctionalization by Radical Alkenyl Migration. *Angew. Chem., Int. Ed.* **2018**, *57*, 814−817. (o) Zhang, Y.; Liu, H.; Tang, L.; Tang, H.-J.; Wang, L.; Zhu, C.; Feng, C.

https://doi.org/10.1021/jacs.2c11867
J. Am. Chem. Soc. XXXX, XXX, XXX−XXX

Intermolecular Carboamination of Unactivated Alkenes. *J. Am. Chem. Soc.* **2018**, *140*, 10695−10699. (p) Nakafuku, K. M.; Fosu, S. C.; Nagib, D. A. Catalytic Alkene Difunctionalization Via Imidate Radicals. *J. Am. Chem. Soc.* **2018**, *140*, 11202−11205. (q) Cheng, Y.; Mück-Lichtenfeld, C.; Studer, A. Transition Metal-Free 1, 2-Carboboration of Unactivated Alkenes. *J. Am. Chem. Soc.* **2018**, *140*, 6221−6225. (r) Shu, W.; García-Domínguez, A.; Quirós, M. T.; Mondal, R.; Cárdenas, D. J.; Nevado, C. Ni-Catalyzed Reductive Dicarbofunctionalization of Nonactivated Alkenes: Scope and Mechanistic Insights. *J. Am. Chem. Soc.* **2019**, *141*, 13812−13821. (s) Wang, X.-G.; Li, Y.; Liu, H.-C.; Zhang, B.-S.; Gou, X.-Y.; Wang, Q.; Ma, J.-W.; Liang, Y.-M. Three-Component Ruthenium-Catalyzed Direct Meta-Selective C−H Activation of Arenes: A New Approach to the Alkylarylation of Alkenes. *J. Am. Chem. Soc.* **2019**, *141*, 13914−13922. (t) Campbell, M. W.; Compton, J. S.; Kelly, C. B.; Molander, G. A. Three-Component Olefin Dicarbofunctionalization Enabled by Nickel/Photoredox Dual Catalysis. *J. Am. Chem. Soc.* **2019**, *141*, 20069−20078. (u) Su, Y.-L.; Liu, G.-X.; Liu, J.-W.; Tram, L.; Qiu, H.; Doyle, M. P. Radical-Mediated Strategies for the Functionalization of Alkenes with Diazo Compounds. *J. Am. Chem. Soc.* **2020**, *142*, 13846−13855. (v) Tu, H.-Y.; Wang, F.; Huo, L.; Li, Y.; Zhu, S.; Zhao, X.; Li, H.; Qing, F.-L.; Chu, L. Enantioselective Three-Component Fluoroalkylarylation of Unactivated Olefins through Nickel-Catalyzed Cross-Electrophile Coupling. *J. Am. Chem. Soc.* **2020**, *142*, 9604−9611. (w) Guo, L.; Yuan, M.; Zhang, Y.; Wang, F.; Zhu, S.; Gutierrez, O.; Chu, L. General Method for Enantioselective Three-Component Carboarylation of Alkenes Enabled by Visible-Light Dual Photoredox/Nickel Catalysis. *J. Am. Chem. Soc.* **2020**, *142*, 20390−20399. (x) Yang, T.; Jiang, Y.; Luo, Y.; Lim, J. J. H.; Lan, Y.; Koh, M. J. Chemoselective Union of Olefins, Organohalides, and Redox-Active Esters Enables Regioselective Alkene Dialkylation. *J. Am. Chem. Soc.* **2020**, *142*, 21410−21419. (y) Liu, W.; Pu, M.; He, J.; Zhang, T.; Dong, S.; Liu, X.; Wu, Y.-D.; Feng, X. Iron-Catalyzed Enantioselective Radical Carboazidation and Diazidation of A, B-Unsaturated Carbonyl Compounds. *J. Am. Chem. Soc.* **2021**, *143*, 11856−11863. (z) Lu, F.-D.; Lu, L.-Q.; He, G.-F.; Bai, J.-C.; Xiao, W.-J. Enantioselective Radical Carbocyanation of 1, 3-Dienes Via Photocatalytic Generation of Allylcopper Complexes. *J. Am. Chem. Soc.* **2021**, *143*, 4168−4173. (aa) Bai, Z.; Zhang, H.; Wang, H.; Yu, H.; Chen, G.; He, G. Enantioselective Alkylamination of Unactivated Alkenes under Copper Catalysis. *J. Am. Chem. Soc.* **2021**, *143*, 1195−1202. (ab) Zhong, T.; Yi, J.-T.; Chen, Z.-D.; Zhuang, Q.-C.; Li, Y.-Z.; Lu, G.; Weng, J. Photoredox-Catalyzed Aminofluorosulfonylation of Unactivated Olefins. *Chem. Sci.* **2021**, *12*, 9359−9365. (ac) Ye, J. H.; Miao, M.; Huang, H.; Yan, S. S.; Yin, Z. B.; Zhou, W. J.; Yu, D. G. Visible-Light-Driven Iron-Promoted Thiocarboxylation of Styrenes and Acrylates with Co2. *Angew. Chem., Int. Ed.* **2017**, *56*, 15416−15420. (ad) Fu, Q.; Bo, Z.-Y.; Ye, J.-H.; Ju, T.; Huang, H.; Liao, L.-L.; Yu, D.-G. Transition Metal-Free Phosphonocarboxylation of Alkenes with Carbon Dioxide Via Visible-Light Photoredox Catalysis. *Nat. Commun.* **2019**, *10*, 3592. (ae) Seefeldt, P.; Dasi, R.; Villinger, A.; Brasholz, M. Photoredox-Induced Deaminative Radical-Cationic Three-Component Couplings with N-Alkylpyridinium Salts and Alkenes. *ChemPhotoChem.* **2021**, *5*, 979−983. (af) Wang, P.-Z.; Liang, Y.-J.; Wu, X.; Guan, W.; Xiao, W.-J.; Chen, J.-R. Copper-Catalyzed Three-Component Photo-Atra-Type Reaction for Asymmetric Intermolecular C−O Coupling. *ACS Catal.* **2022**, *12*, 10925−10937. (ag) Yan, D.-M.; Xu, S.-H.; Qian, H.; Gao, P.-P.; Bi, M.-H.; Xiao, W.-J.; Chen, J.-R. Photoredox-Catalyzed and Copper (Ii) Salt-Assisted Radical Addition/Hydroxylation Reaction of Alkenes, Sulfur Ylides, and Water. *ACS Catal.* **2022**, *12*, 3279−3285. (ah) Wang, P.-Z.; Gao, Y.; Chen, J.; Huan, X.-D.; Xiao, W.-J.; Chen, J.-R. Asymmetric Three-Component Olefin Dicarbofunctionalization Enabled by Photoredox and Copper Dual Catalysis. *Nat. Commun.* **2021**, *12*, 1815. (ai) Jia, X.-G.; Yao, Q.-W.; Shu, X.-Z. Enantioselective Reductive N-Cyclization−Alkylation Reaction of Alkene-Tethered Oxime Esters and Alkyl Iodides by Nickel Catalysis. *J. Am. Chem. Soc.* **2022**, *144*, 13461−13467. (aj) Bian, K.-J.; Nemoto, D., Jr; Kao, S.-C.; He, Y.; Li, Y.; Wang, X.-S.; West, J. G. Modular Difunctionalization of Unactivated Alkenes through Bio-Inspired Radical Ligand Transfer Catalysis. *J. Am. Chem. Soc.* **2022**, *144*, 11810−11821. (ak) Cheng, X.-Y.; Zhang, Y.-F.; Wang, J.-H.; Gu, Q.-S.; Li, Z.-L.; Liu, X.-Y. A Counterion/Ligand-Tuned Chemo-and Enantioselective Copper-Catalyzed Intermolecular Radical 1, 2-Carboamination of Alkenes. *J. Am. Chem. Soc.* **2022**, *144*, 18081−18089.

(4) (a) Jana, K.; Bhunia, A.; Studer, A. Radical 1, 3-Difunctionalization of Allylboronic Esters with Concomitant 1, 2-Boron Shift. *Chem.* **2020**, *6*, 512−522. (b) Li, Z.; Wang, M.; Shi, Z. Radical Addition Enables 1, 2-Aryl Migration from a Vinyl-Substituted All-Carbon Quaternary Center. *Angew. Chem., Int. Ed.* **2021**, *60*, 186−190. (c) Zhang, Q.; Chiou, M.-F.; Ye, C.; Yuan, X.; Li, Y.; Bao, H. Radical 1, 2, 3-Tricarbofunctionalization of A-Vinyl-B-Ketoesters Enabled by a Carbon Shift from an All-Carbon Quaternary Center. *Chem. Sci.* **2022**, *13*, 6836−6841.

(5) For a selected review, see: (a) Beckwith, A. L. J.; Crich, D.; Duggan, P. J.; Yao, Q. Chemistry of B-(Acyloxy)Alkyl and B-(Phosphatoxy)Alkyl Radicals and Related Species: Radical and Radical Ionic Migrations and Fragmentations of Carbon−Oxygen Bonds. *Chem. Rev.* **1997**, *97*, 3273−3312. For original reports, see: (b) Surzur, J.; Teissier, P. Addition Radicalaire Desters Sur Les Alcools Ethyleniques. *C. R. Acad. Sci. Fr. Ser. C* **1967**, *264*, 1981−1984. (c) Tanner, D. D.; Law, F. C. Free-Radical Acetoxy Group Migration. *J. Am. Chem. Soc.* **1969**, *91*, 7535−7537.

(6) For selected recent reviews, see: (a) Guo, H.; Fan, Y. C.; Sun, Z.; Wu, Y.; Kwon, O. Phosphine Organocatalysis. *Chem. Rev.* **2018**, *118*, 10049−10293. (b) Rossi-Ashton, J. A.; Clarke, A. K.; Unsworth, W. P.; Taylor, R. J. Phosphoranyl Radical Fragmentation Reactions Driven by Photoredox Catalysis. *ACS Catal.* **2020**, *10*, 7250−7261. (c) Hu, X.-Q.; Hou, Y.-X.; Liu, Z.-K.; Gao, Y. Recent Advances in Phosphoranyl Radical-Mediated Deoxygenative Functionalisation. *Org. Chem. Front.* **2020**, *7*, 2319−2324. (d) Xie, C.; Smaligo, A. J.; Song, X.-R.; Kwon, O. Phosphorus-Based Catalysis. *ACS Cent. Sci.* **2021**, *7*, 536−558. (e) Maddigan-Wyatt, J.; Hooper, J. F. Phosphorus Compounds as Precursors and Catalysts for Radical C−C Bond-Forming Reactions. *Adv. Synth. Catal.* **2021**, *363*, 924−936. (f) Khong, S.; Venkatesh, T.; Kwon, O. Nucleophilic Phosphine Catalysis: The Untold Story. *Asian J. Org. Chem.* **2021**, *10*, 2699−2708. (g) Lipshultz, J. M.; Li, G.; Radosevich, A. T. Main Group Redox Catalysis of Organopnictogens: Vertical Periodic Trends and Emerging Opportunities in Group 15. *J. Am. Chem. Soc.* **2021**, *143*, 1699−1721.

(7) (a) Zhang, K.; Cai, L.; Jiang, X.; Garcia-Garibay, M. A.; Kwon, O. Phosphine-Mediated Iterative Arene Homologation Using Allenes. *J. Am. Chem. Soc.* **2015**, *137*, 11258−11261. (b) Hilton, M. C.; Dolewski, R. D.; McNally, A. Selective Functionalization of Pyridines Via Heterocyclic Phosphonium Salts. *J. Am. Chem. Soc.* **2016**, *138*, 13806−13809. (c) Hilton, M. C.; Zhang, X.; Boyle, B. T.; Alegre-Requena, J. V.; Paton, R. S.; McNally, A. Heterobiaryl Synthesis by Contractive C−C Coupling Via P (V) Intermediates. *Science* **2018**, *362*, 799−804. (d) Nykaza, T. V.; Cooper, J. C.; Li, G.; Mahieu, N.; Ramirez, A.; Luzung, M. R.; Radosevich, A. T. Intermolecular Reductive C-N Cross Coupling of Nitroarenes and Boronic Acids by P(III)/P(V)=O Catalysis. *J. Am. Chem. Soc.* **2018**, *140*, 15200−15205. (e) Wang, H.; Zhang, L.; Tu, Y.; Xiang, R.; Guo, Y. L.; Zhang, J. Phosphine-Catalyzed Difunctionalization of β-Fluoroalkyl α,β-Enones: A Direct Approach to β-Amino α-Diazo Carbonyl Compounds. *Angew. Chem., Int. Ed.* **2018**, *57*, 15787−15791. (f) Beddoe, R. H.; Andrews, K. G.; Magné, V.; Cuthbertson, J. D.; Saska, J.; Shannon-Little, A. L.; Shanahan, S. E.; Sneddon, H. F.; Denton, R. M. Redox-Neutral Organocatalytic Mitsunobu Reactions. *Science* **2019**, *365*, 910−914. (g) Cai, L.; Zhang, K.; Chen, S.; Lepage, R. J.; Houk, K.; Krenske, E. H.; Kwon, O. Catalytic Asymmetric Staudinger−Aza-Wittig Reaction for the Synthesis of Heterocyclic Amines. *J. Am. Chem. Soc.* **2019**, *141*, 9537−9542. (h) Chan, W. L.; Tang, X.; Zhang, F.; Quek, G.; Mei, G. J.; Lu, Y. Phosphine-Catalyzed (3 + 2) Annulation of Isoindigos with Allenes: Enantioselective Formation of Two Vicinal Quaternary Stereogenic Centers. *Angew. Chem.* **2019**, *131*, 6326−6330. (i) Chen, X.; Gao, D.; Wang, D.; Xu,

https://doi.org/10.1021/jacs.2c11867
J. Am. Chem. Soc. XXXX, XXX, XXX−XXX

T.; Liu, W.; Tian, P.; Tong, X. Access to Aryl-Naphthaquinone Atropisomers by Phosphine-Catalyzed Atroposelective (4 + 2) Annulations of Δ-Acetoxy Allenoates with 2-Hydroxyquinone Derivatives. *Angew. Chem.* **2019**, *131*, 15478−15482. (j) Ghosh, A.; Lecomte, M.; Kim-Lee, S. H.; Radosevich, A. T. Organophosphorus-Catalyzed Deoxygenation of Sulfonyl Chlorides: Electrophilic (Fluoroalkyl) Sulfenylation by P(III)/P(V)=O Redox Cycling. *Angew. Chem., Int. Ed.* **2019**, *58*, 2864−2869. (k) He, X.; Tang, Y.; Wang, Y.; Chen, J. B.; Xu, S.; Dou, J.; Li, Y. Phosphine-Catalyzed Activation of Alkylidenecyclopropanes: Rearrangement to Form Polysubstituted Furans and Dienones. *Angew. Chem.* **2019**, *131*, 10808−10812. (l) Lecomte, M.; Lipshultz, J. M.; Kim-Lee, S.-H.; Li, G.; Radosevich, A. T. Driving Recursive Dehydration by Piii/Pv Catalysis: Annulation of Amines and Carboxylic Acids by Sequential C−N and C−C Bond Formation. *J. Am. Chem. Soc.* **2019**, *141*, 12507−12512. (m) Lorton, C.; Castanheiro, T.; Voituriez, A. Catalytic and Asymmetric Process Via P(III)/P(V)=O Redox Cycling: Access to (Trifluoromethyl) Cyclobutenes Via a Michael Addition/Wittig Olefination Reaction. *J. Am. Chem. Soc.* **2019**, *141*, 10142−10147. (n) Mato, R.; Manzano, R. n.; Reyes, E.; Carrillo, L.; Uria, U.; Vicario, J. L. Catalytic Enantioselective Transannular Morita−Baylis−Hillman Reaction. *J. Am. Chem. Soc.* **2019**, *141*, 9495−9499. (o) Wu, M.; Han, Z.; Li, K.; Wu, J. e.; Ding, K.; Lu, Y. Cyclohexyl-Fused, Spirobiindane-Derived, Phosphine-Catalyzed Synthesis of Tricyclic Γ-Lactams and Kinetic Resolution of Γ-Substituted Allenoates. *J. Am. Chem. Soc.* **2019**, *141*, 16362−16373. (p) Cao, Z. H.; Wang, Y. H.; Kalita, S. J.; Schneider, U.; Huang, Y. Y. Phosphine-Catalyzed [4+ 1] Cycloadditions of Allenes with Methyl Ketimines, Enamines, and a Primary Amine. *Angew. Chem., Int. Ed.* **2020**, *59*, 1884−1890. (q) Li, G.; Nykaza, T. V.; Cooper, J. C.; Ramirez, A.; Luzung, M. R.; Radosevich, A. T. An Improved P(III)/P(V)=O-Catalyzed Reductive C−N Coupling of Nitroaromatics and Boronic Acids by Mechanistic Differentiation of Rate-and Product-Determining Steps. *J. Am. Chem. Soc.* **2020**, *142*, 6786−6799. (r) Longwitz, L.; Werner, T. Reduction of Activated Alkenes by P(III)/P(V) Redox Cycling Catalysis. *Angew. Chem., Int. Ed.* **2020**, *59*, 2760−2763.

(8) (a) Yu, P.; Zheng, S. C.; Yang, N. Y.; Tan, B.; Liu, X. Y. Phosphine-Catalyzed Remote *β*-C-H Functionalization of Amines Triggered by Trifluoromethylation of Alkenes: One-Pot Synthesis of Bistrifluoromethylated Enamides and Oxazoles. *Angew. Chem., Int. Ed.* **2015**, *54*, 4041−4045. (b) Li, L.; Ye, L.; Ni, S.-F.; Li, Z.-L.; Chen, S.; Du, Y.-M.; Li, X.-H.; Dang, L.; Liu, X.-Y. Phosphine-Catalyzed Remote A-C−H Bond Activation of Alcohols or Amines Triggered by the Radical Trifluoromethylation of Alkenes: Reaction Development and Mechanistic Insights. *Org. Chem. Front.* **2017**, *4*, 2139−2146. (c) Lu, H.; Wang, D.-y.; Zhang, A. Visible Light-Promoted Phosphine-Catalyzed Difluoroalkylation of Arenes and Heterocycles. *J. Org. Chem.* **2020**, *85*, 942−951. (d) Zhao, L.; Huang, Y.; Wang, Z.; Zhu, E.; Mao, T.; Jia, J.; Gu, J.; Li, X.-F.; He, C.-Y. Organophosphine-Catalyzed Difluoroalkylation of Alkenes. *Org. Lett.* **2019**, *21*, 6705−6709. (e) Helmecke, L.; Spittler, M.; Baumgarten, K.; Czekelius, C. Metal-Free Activation of C−I Bonds and Perfluoroalkylation of Alkenes with Visible Light Using Phosphine Catalysts. *Org. Lett.* **2019**, *21*, 7823−7827. (f) Fu, M.-C.; Shang, R.; Zhao, B.; Wang, B.; Fu, Y. Photocatalytic Decarboxylative Alkylations Mediated by Triphenylphosphine and Sodium Iodide. *Science* **2019**, *363*, 1429−1434. (g) Wang, Y.-T.; Fu, M.-C.; Zhao, B.; Shang, R.; Fu, Y. Photocatalytic Decarboxylative Alkenylation of A-Amino and A-Hydroxy Acid-Derived Redox Active Esters by Nai/Pph 3 Catalysis. *Chem. Commun.* **2020**, *56*, 2495−2498. (h) Fu, M.-C.; Wang, J.-X.; Shang, R. Triphenylphosphine-Catalyzed Alkylative Iododecarboxylation with Lithium Iodide under Visible Light. *Org. Lett.* **2020**, *22*, 8572−8577. (i) Liu, C.; Shen, N.; Shang, R. Photocatalytic Defluoroalkylation and Hydrodefluorination of Trifluoromethyls Using O-Phosphinophenolate. *Nat. Commun.* **2022**, *13*, 354. (j) Shen, N.; Li, R.; Liu, C.; Shen, X.; Guan, W.; Shang, R. Photocatalytic Cross-Couplings of Aryl Halides Enabled by O-Phosphinophenolate and *o*-Phosphinothiophenolate. *ACS Catal.* **2022**, *12*, 2788−2795.

(9) Juliá, F.; Constantin, T.; Leonori, D. Applications of Halogen-Atom Transfer (XAT) for the Generation of Carbon Radicals in Synthetic Photochemistry and Photocatalysis. *Chem. Rev.* **2022**, *122*, 2292−2352.

(10) (a) Lima, C. G.; de M. Lima, T.; Duarte, M.; Jurberg, I. D.; Paixao, M. W. Organic Synthesis Enabled by Light-Irradiation of Eda Complexes: Theoretical Background and Synthetic Applications. *ACS Catal.* **2016**, *6*, 1389−1407. (b) Postigo, A. Electron Donor-Acceptor Complexes in Perfluoroalkylation Reactions. *Eur. J. Org. Chem.* **2018**, *2018*, 6391−6404. (c) Crisenza, G. E.; Mazzarella, D.; Melchiorre, P. Synthetic Methods Driven by the Photoactivity of Electron Donor-Acceptor Complexes. *J. Am. Chem. Soc.* **2020**, *142*, 5461−5476. (d) Yuan, Y.-q.; Majumder, S.; Yang, M.-h.; Guo, S.-r. Recent Advances in Catalyst-Free Photochemical Reactions Via Electron-Donor-Acceptor (EDA) Complex Process. *Tetrahedron Lett.* **2020**, *61*, 151506.

(11) (a) Bracker, M.; Helmecke, L.; Kleinschmidt, M.; Czekelius, C.; Marian, C. M. Visible Light-Induced Homolytic Cleavage of Perfluoroalkyl Iodides Mediated by Phosphines. *Molecules* **2020**, *25*, 1606. (b) Wulkesch, C.; Czekelius, C. Straightforward Synthesis of Fluorinated Enals Via Photocatalytic A-Perfluoroalkenylation of Aldehydes. *J. Org. Chem.* **2021**, *86*, 7425−7438.

(12) The computed LUMO energies of bromodifluoroacetate and iododifluoroacetate are −41.8 and −53.3 kcal/mol, respectively; see the Supporting Information for details.

(13) (a) Böhm, H. J.; Banner, D.; Bendels, S.; Kansy, M.; Kuhn, B.; Müller, K.; Obst-Sander, U.; Stahl, M. Fluorine in Medicinal Chemistry. *ChemBioChem.* **2004**, *5*, 637−643. (b) Muller, K.; Faeh, C.; Diederich, F. Fluorine in Pharmaceuticals: Looking Beyond Intuition. *Science* **2007**, *317*, 1881−1886. (c) Gillis, E. P.; Eastman, K. J.; Hill, M. D.; Donnelly, D. J.; Meanwell, N. A. Applications of Fluorine in Medicinal Chemistry. *J. Med. Chem.* **2015**, *58*, 8315−8359. (d) Meanwell, N. A. Fluorine and Fluorinated Motifs in the Design and Application of Bioisosteres for Drug Design. *J. Med. Chem.* **2018**, *61*, 5822−5880. (e) Ogawa, Y.; Tokunaga, E.; Kobayashi, O.; Hirai, K.; Shibata, N. Current Contributions of Organofluorine Compounds to the Agrochemical Industry. *iScience* **2020**, *23*, 101467. (f) Inoue, M.; Sumii, Y.; Shibata, N. Contribution of Organofluorine Compounds to Pharmaceuticals. *Acs Omega* **2020**, *5*, 10633−10640.

(14) Prices obtained from Sigma Aldrich as of October 2022.

(15) Na_2CO_3 could serve as a base to prevent catalyst deactivation and/or form an adduct with dppm−**2a** complex to promote photoexcitation; see Figures S14−S16 in the Supporting Information.

(16) Cernak, T.; Dykstra, K. D.; Tyagarajan, S.; Vachal, P.; Krska, S. W. The Medicinal Chemist's Toolbox for Late Stage Functionalization of Drug-Like Molecules. *Chem. Soc. Rev.* **2016**, *45*, 546−576.

(17) Legault, C. Y. *Cylview20*; Université De Sherbrooke: 2020; http://www.cylview.org (accessed January 18, 2023).

(18) Zhao, G.; Yao, W.; Mauro, J. N.; Ngai, M. Y. Excited-State Palladium-Catalyzed 1,2-Spin-Center Shift Enables Selective C-2 Reduction, Deuteration, and Iodination of Carbohydrates. *J. Am. Chem. Soc.* **2021**, *143*, 1728−1734.

(19) An alternative mechanism is the heterolytic fragmentation to form transient radical cations followed by recombination. See: Horner, J. H.; Bagnol, L.; Newcomb, M. Kinetics of Radical Heterolysis Reactions Forming Alkene Radical Cations. *J. Am. Chem. Soc.* **2004**, *126*, 14979−14987. However, DFT calculations showed that the formation of benzoate and the corresponding radical cation from **IV** is more than 23 kcal/mol higher than the concerted [1,2]- and [2,3]-transition states. See the Supporting Information for details.

(20) (a) Job, P. A Job Plot Is Used to Determine Stoichiometry. *Ann. Chim. (Paris)* **1928**, *9*, 113−203. (b) Wang, Y.; Wang, J.; Li, G.-X.; He, G.; Chen, G. Halogen-Bond-Promoted Photoactivation of Perfluoroalkyl Iodides: A Photochemical Protocol for Perfluoroalkylation Reactions. *Org. Lett.* **2017**, *19*, 1442−1445.

(21) Benesi, H. A.; Hildebrand, J. A Spectrophotometric Investigation of the Interaction of Iodine with Aromatic Hydrocarbons. *J. Am. Chem. Soc.* **1949**, *71*, 2703−2707.

https://doi.org/10.1021/jacs.2c11867
J. Am. Chem. Soc. XXXX, XXX, XXX−XXX

(22) For an example of phosphine−Cs_2CO_3 adducts, see: Guo, Z.; Li, M.; Mou, X.-Q.; He, G.; Xue, X.-S.; Chen, G. Radical C−H Arylation of Oxazoles with Aryl Iodides: Dppf as an Electron-Transfer Mediator for Cs_2co_3. *Org. Lett.* **2018**, *20*, 1684−1687. Our system likely behaves differently from this mechanism because we did not observe the formation of phosphine oxide and 2,6-lutidine can promote the desired reaction as well.

(23) For Lewis-base-promoted photolysis, see: Fang, C.-Z.; Zhang, B.-B.; Li, B.; Wang, Z.-X.; Chen, X.-Y. Water facilitated photolysis of perfluoroalkyl iodides via halogen bonding. *Org. Chem. Front.* **2022**, *9*, 2579−2584. DFT calculations showed that the cleavage of the C−Br bond through SET from phosphine catalyst to σ^* of C−Br is energetically more favorable in our case.

(24) Although the Br-atom transfer from the P−Br radical has not been reported, an analogous I-atom transfer from the P−I radical to the alkyl radical has been proposed; see refs 6e and 8h.

https://doi.org/10.1021/jacs.2c11867
J. Am. Chem. Soc. XXXX, XXX, XXX−XXX